Available online at www.sciencedirect.com
ScienceDirect
Journal of Nuclear Materials 366 (2007) 70–86
journal of nuclear materials
www.elsevier.com/locate/jnucmat

Synthesis and characterization of uranium-bearing britholites

Olivier Terra [a], Fabienne Audubert [b], Nicolas Dacheux [a,*], Christophe Guy [c], Renaud Podor [d]

[a] Groupe de Radiochimie, IPN Orsay, Bât. 100, Université de Paris-Sud-11, 91406 Orsay, France
[b] CEA Cadarache, DEN/DEC/SPUA/LTEC, Bât. 307, 13108 Saint Paul Lez Durance, France
[c] CEA Cadarache, DEN/DEC/SA3C/LARC, Bât. 152, 13108 Saint Paul Lez Durance, France
[d] LCSM (CNRS UMR 7555), Université H. Poincaré-Nancy I, BP 239, 54506 Vandœuvre lès Nancy, France

Received 1 September 2006; accepted 15 December 2006

Abstract

Unlike thorium which incorporation is easy and quantitative in the britholite structure, that of tetravalent uranium appears rather difficult even after heating at high temperature. Indeed, only about 3.5 wt% of uranium (instead of 10.3 wt% expected) are incorporated in the britholite structure when using a manual grinding of the initial mixture while it is increased to 5.9 wt% when performing mechanical grinding/heating cycles. The optimized grinding and heating conditions can be fixed to 15 min at 30 Hz and to 1400 °C for 6 h, respectively. All the samples prepared at 1400 °C are found to be composed by (Nd, U)-britholite and calcium uranate CaU_2O_{5+y} which formation results from that of $CaUO_4$ above 800 °C consequently to the direct reaction between UO_2 and CaO. The incorporation of tetravalent uranium in (Nd, U)-britholites begins simultaneously to the transformation of $CaUO_4$ into CaU_2O_{5+y} above 1100 °C. Due to these redox reactions, the incorporation of uranium remains partial even though it is significantly increased at 1400 °C and mainly proceeds through diffusion phenomena. Two main methods can be used to improve significantly the incorporation of uranium in (Nd, U)-britholites. The first one deals with the compaction of the powdered initial mixture prior to perform the heating treatment at 1400 °C. The second one is based on the simultaneous incorporation of tetravalent thorium and uranium, leading to the formation of (Nd, Th, U)-britholites. Like for uranium, such methods could be of significant interest in the field of the incorporation of other tetravalent actinides, e.g. neptunium or plutonium, which could be also stabilized in several oxidation states.

1. Introduction

As already discussed, several ceramics were proposed as good candidates for the immobilization of minor actinides such as Np, Am or Cm [1–3] in the framework of long-term storage of long life radionuclides. In this scope, the French national research group NOMADE has initiated a multidisciplinary program of evaluation that allowed to select host ceramics for their high chemical durability, their low aqueous solubility and their resistance to radiation damage [1]. On the basis of preliminary results, several materials were thus proposed as suitable host matrices: zirconolites $(Ca_{1-x}Nd_x)ZrTi_{2-x}Al_xO_7$,

* Corresponding author. Tel.: +33 1 69 15 73 46; fax: +33 1 69 15 71 50.
E-mail address: dacheux@ipno.in2p3.fr (N. Dacheux).

0022-3115/$ - see front matter © 2007 Elsevier B.V. All rights reserved.
doi:10.1016/j.jnucmat.2006.12.047

monazite/brabantite solid solutions $Ln^{III}_{1-2x}Ca_xAn^{IV}_xPO_4$ [4–6], thorium phosphate diphosphate β-$Th_4(PO_4)_4P_2O_7$ [7–9], associated solid solutions [10–14] or combinations with monazites [15] and finally britholites $Ca_9Nd(PO_4)_5(SiO_4)F_2$ [16,17].

This latter phase can be considered as a host matrix for the immobilization of either trivalent or tetravalent actinides [18]. Indeed, in natural apatites (particularly those coming from the Oklo fossil nuclear reactors – Gabon), the structure has been able to accept a large variety of cationic substitutions, leading to the simultaneous incorporation of lanthanides, thorium and uranium [19,20]. Furthermore, some samples of silicate-based apatite (britholites) of In Ouzzal site (Algeria) were found to contain up to 50 wt% of actinides (U, Th) [21].

Moreover, the apatite structure seems to be able to anneal the defects generated by self-irradiation even at low temperature [22]. However, it has been also proved that the metamictization process (destruction of the crystal lattice due to radiation damage) strongly depends on the chemical composition of the apatites [22]. For this reason, the mono-silicated britholite $Ca_9Nd(PO_4)_5(SiO_4)F_2$ (in which neodymium is used as a surrogate of trivalent actinides) was considered as the starting material [18].

Since natural analogues and external irradiation studies clearly identified the mono-silicated fluorapatite as a potential waste form [18,23] and since the synthesis and sintering of Nd-bearing britholite was already established [24–26], we chose to focus our work on the incorporation of tetravalent actinides (such as Th,U) in britholites.

A lot of natural thorium bearing apatites was sampled in the field of the Th–U thermochronology [27–29]. The incorporation of thorium in synthetic britholite samples was first studied through the preparation of the full-silicated apatite $Ca_6Th_4(SiO_4)_6O_2$ [30]. More recently, we reported the preparation of (Nd, Th)-britholites, of general formula $Ca_9Nd_{1-x}Th_x(PO_4)_{5-x}(SiO_4)_{1+x}F_2$, from several thorium reagents (mainly oxides and phosphates) [17]. The use of mechanical grinding steps (15 min, 30 Hz) allowed to increase the specific surface area (thus the reactivity) of the mixture and led to a better homogeneity of the final samples. The thorium incorporation occurred above 1100 °C. Nevertheless, it was necessary to fire the initial mixture at 1400 °C for 6 h to prepare single phase and homogeneous compounds. In order to ensure the quantitative incorporation of thorium, it appeared necessary to consider the coupled substitution $(Nd^{3+}, PO_4^{3-}) \Longleftrightarrow (Th^{4+}, SiO_4^{4-})$ instead of $(Nd^{3+}, F^-) \Longleftrightarrow (Th^{4+}, O^{2-})$. By using this method, homogeneous and single phase solid solutions were prepared from $Ca_9Nd(PO_4)_5(SiO_4)F_2$ to $Ca_9Th(PO_4)_4(SiO_4)_2F_2$ leading to the whole neodymium substitution. The associated small increase of the unit cell parameters observed results from the simultaneous replacement of phosphate by bigger silicate groups.

These results contrast with that obtained when using the coupled substitution $(Nd^{3+}, F^-) \Longleftrightarrow (Th^{4+}, O^{2-})$ which led to a limitation of about 10 wt% in the thorium substitution, the samples being polyphase for higher values due to problems in the charge balance consequently to the partial substitution of fluoride by oxide ions. On the basis of the results reported in this paper, the sintering of (Nd, Th)-britholite (with $x = 0.5$) was thus undertaken in order to perform the densification of the samples then several physico-chemical properties of the pellets, such as the chemical durability during leaching tests, were examined [16].

According to literature, the incorporation of uranium in the apatite structure was already tried several times in the last years from both stable oxidation states U(VI) and U(IV). The results were particularly interesting when using hexavalent uranium. Rakovan et al. [31] reported the incorporation of U(VI) under the hexapositive form U^{6+} in the fluoroapatite $Ca_{9.9}U_{0.1}(PO_4)_6F_{1.8}$ corresponding to 2.2 wt% (U). The synthesis was carried out by firing a mixture of UO_2, $Ca_3(PO_4)_2$ and CaF_2 at 1380 °C in air. XANES and EXAFS analyses were also performed to confirm the presence of U^{6+} (instead of the uranyl groups UO_2^{2+}).

Vance et al. [32] studied the incorporation of uranium in phosphate-based or silicate-based apatites. In the frame of synthesis of $Ca_9Gd_{0.33}U_{0.33}(PO_4)_5(SiO_4)O$ under inert atmosphere at 1300–1400 °C, the polyphase system obtained was composed by $Ca_3(PO_4)_2$, $(U,Ca,Gd)O_{2-x}$ fluorite-type structure and apatite loaded with 0.5 atom per formula unit. Afterwards, Vance et al. [33] tried to prepared a full-silicated compound. They obtained a britholite with a composition of $Ca_2Gd_7U_{0.33}(SiO_4)_6O_2$ after heating at 1350 °C under inert or reducing atmosphere (H_2–3.5%/N_2).

More recently, the incorporation of uranium was also studied in a britholite with general formula $Ca_a La_b U_x(PO_4)_3(SiO_4)_3O_c$ (with $a + b + x = 10$, a and b near to 5 and $0 \leqslant x \leqslant 0.8$). El Ouenzerfi et al.

[34] established that a limit of incorporation of 0.48 atom per formula unit was obtained in the apatite structure. The authors underlined that for higher incorporation rates, the excess of uranium was present as UO_2 and U_3O_8. Nevertheless, El Ouenzerfi et al. proved that the uranium incorporated in the britholite structure was present in the tetravalent oxidation state since μ-Raman spectra did not indicate the presence of uranyl units (UO_2^{2+}).

In our study, the limit of incorporation of uranium was first fixed to 10 wt%. As neodymium is used as a surrogate of trivalent actinide, we partly substituted trivalent neodymium by tetravalent uranium using the coupled substitution $(Nd^{3+}, PO_4^{3-}) \Longleftrightarrow (U^{4+}, SiO_4^{4-})$ in the aim to prepare $Ca_9Nd_{1-x}U_x(PO_4)_{5-x}(SiO_4)_{1+x}F_2$ compounds. On the basis of the difficulties reported during the preparation of (Nd, Th)-britholites [17], the coupled substitution $(Nd^{3+}, F^-) \Longleftrightarrow (U^{4+}, O^{2-})$ was not considered thereafter. Even though (Nd, U)-britholites were synthesized from several uranium reagents, we thus focused the study on the use of uranium dioxide to follow the incorporation of this element in the britholite structure. On the basis of the results obtained during the synthesis of (Nd, Th)-britholites [17] and thanks to the understanding of the incorporation of uranium in the britholite structure, we tried to optimize the incorporation rate of uranium up to the 10 wt% expected.

In order to simplify the notation, britholites loaded with neodymium (e.g. $Ca_9Nd(PO_4)_5(SiO_4)F_2$) will be noted Nd-britholite and those which simultaneously contain neodymium and uranium (i.e. $Ca_9Nd_{1-x}U_x(PO_4)_{5-x}(SiO_4)_{1+x}F_2$) will be called (Nd, U)-britholite. In most of the cases, this notation will be used for x value equal to 0.5. For other compositions, the x values will be given when necessary.

2. Experimental

2.1. Preparation of the samples

All the chemicals used for the synthesis (e.g. Nd_2O_3, CaF_2, UO_2, $Ca(HPO_4) \cdot 2H_2O$, SiO_2, $CaCO_3$) were of pro-analysis grade. Samples of (Nd, U)-britholites were prepared through dry chemistry methods involving an initial mixture of $Nd_2O_3/Ca_2P_2O_7/CaCO_3/CaF_2/SiO_2/UO_2$ according to the global reaction:

$$\frac{1}{4}Nd_2O_3 + \frac{9}{4}Ca_2P_2O_7 + \frac{7}{2}CaCO_3 + CaF_2 + \frac{3}{2}SiO_2 + \frac{1}{2}UO_2 \rightarrow Ca_9Nd_{0.5}U_{0.5}(PO_4)_{4.5}(SiO_4)_{1.5}F_2 + \frac{7}{2}CO_2 \uparrow \quad (1)$$

Prior to perform the synthesis, neodymium oxide was first heated at 1000 °C for 3 h to eliminate the presence of neodymium hydroxide. Calcium diphosphate was prepared from $Ca(HPO_4) \cdot 2H_2O$ by heating at 1000 °C for 3 h. For several syntheses, CaO was also used instead of $CaCO_3$ because this latter is responsible of a significant agglomeration of the grains which was found to degrade the efficiency of the following grinding step prior to perform the sintering process.

The capability of uranium to be incorporated in the britholite structure was evaluated from several reagents. They were mainly UO_2 (prepared by calcination of $U(C_2O_4)_2 \cdot nH_2O$ at 1000 °C for 10 h) or phosphates (e.g. α-UP_2O_7 or UPHPH: $U_2(PO_4)_2(HPO_4) \cdot H_2O) \cdot$ α-UP_2O_7 was prepared from a mixture of UCl_4 and H_3PO_4 concentrated solutions in the mole ratio $U/P = 1/2$ after the complete evaporation of the mixture then heating at 800 °C for 12 h. Crystallized UPHPH was prepared through precipitation from the same mixture of concentrated solutions ($t = 7$ days, $T = 150$ °C, close container) considering a mole ratio U/P equal to 2/3, after washing with ethanol then drying. As an example, the reaction considered from uranium diphosphate can be written as:

$$\frac{1}{4}Nd_2O_3 + \frac{7}{4}Ca_2P_2O_7 + \frac{9}{2}CaCO_3 + CaF_2 + \frac{3}{2}SiO_2 + \frac{1}{2}\alpha\text{-}UP_2O_7 \rightarrow Ca_9Nd_{0.5}U_{0.5}(PO_4)_{4.5}(SiO_4)_{1.5}F_2 + \frac{9}{2}CO_2 \uparrow \quad (2)$$

Previous studies showed that the incorporation of neodymium as Nd-britholite was not still complete at 1200 °C when using a manual grinding. Above this temperature, neodymium and silicate ions participated to the formation of the britholite structure [17,35]. In the case of the preparation of (Nd, Th)-britholites samples [17], the incorporation of both elements occurred above 1100 °C thanks to the use of mechanical grinding steps. The mechanism of incorporation of uranium could be similar.

Consequently, two kinds of syntheses were performed: the first one involved manual grinding steps of the powders in acetone for 15 min. It was followed by evaporation of the solvent. The second one was based on mechanical grindings of the powders in a zircon crusher. Indeed, as already shown for (Nd, Th)-britholites, the manual grinding always led to less homogeneous samples than using mechanical grinding of the initial reagents. For this reason, the major part of the samples was prepared through grinding/calcination steps. The frequency of the oscillations of the crusher (RETSCH MM200) varied from 0 to 30 Hz, depending on the grinding efficiency expected. All the grinding steps were realized for cycles of 15 min. The ground mixtures were thus heated at 1400 °C for 6 h under inert atmosphere in a PYROX HM 40 furnace with heating and cooling rates of 5 °C min^{-1}.

In order to avoid any reaction between silica and alumina, which was observed during a first series of preparation of (Nd, Th)-britholites [17], all the powders were heated in platinum boats or in alumina boats covered by platinum.

2.2. Characterization

The X-ray powder diffraction (XRD) patterns were collected with a Bruker AXS D8 Advance diffractometer system using Cu Kα rays ($\lambda = 1.5418$ Å).

The electron probe microanalyses (EPMA) and X-EDS mapping were carried out using Cameca SX 50 and SX 100 probes (operating with an acceleration voltage of 15 kV and a current intensity of 10 nA). The calibration standards used were mainly topaze $Al_2SiO_4F_2$ (Kα ray of fluorine), orthose $KAlSi_3O_8$ (Kα ray of silicon), $LaPO_4$ and $NdPO_4$ monazites (Kα ray of phosphorus and Lα ray of neodymium, respectively), wollastonite Ca_2SiO_4 (Kα ray of calcium), ThO_2 (Mα ray of thorium) and $UO_{2.12}$ (Mβ ray of uranium). Some interferences were also detected during EPMA analyses in the samples containing simultaneously large amounts of calcium and uranium, leading to an overestimation of calcium as already discussed for other compounds like $Ca_{0.5}Th_{0.5-x}U_xPO_4$ brabantites [36]. Scanning Electron Microscopy (SEM) studies were carried out with a Hitachi S2500 scanning electron microscope.

Infrared absorption spectra were carried out on a spectrophotometer HITACHI I-2001 ranging from 400 to 4000 cm^{-1}. The solids were dispersed in pellets of KBr with a weight percent of 1–2%. μ-Raman spectra were recorded with a microspectrometer LABRAM (Dilor – Jobin Yvon) using an argon laser (514.5 nm). The laser source, which power varied from 1 to 10 mW, was positioned on the sample thanks to an Olympus microscope.

3. Results and discussion

3.1. Incorporation of uranium versus the heating temperature

3.1.1. Characterization by XRD and electron probe microanalyses

In order to understand the mechanism driving the incorporation of uranium in britholites, especially in the field of its comparison to that of thorium in (Nd, Th)-britholites [17], the behavior of uranium was followed versus the heating temperature using dry chemical processes from a mixture of powdered Nd_2O_3, $Ca_2P_2O_7$, $CaCO_3$, CaF_2, SiO_2 and UO_2 with the aim to prepare samples of $Ca_9Nd_{0.5}U_{0.5}(PO_4)_{4.5}(SiO_4)_{1.5}F_2$. On the basis of the optimized conditions reported for (Nd, Th)-britholites [17], the mixture was mechanically ground for 15 min at a frequency of 30 Hz, then heated between 800 and 1400 °C for 6 h.

After each heating step, the powders were characterized by using XRD and EPMA. The XRD patterns are reported in Fig. 1 for $800 \leqslant T \leqslant 1400$ °C, while the corresponding refined unit cell parameters are gathered in Table 1 and in Fig. 2. The variation of the chemical composition of associated samples determined from EPMA experiments is reported in Fig. 3.

From this study, the first important point to be evoked concerns the change in colour of the powders. Indeed, while the initial mixture presents a black colour characteristic to the presence of UO_2 in the mixture, it turns to a yellow coloured between 800 and 1000 °C then finally to dark-green then black above 1100 °C. These observations clearly traduce several valence changes during the syntheses with uranium and, consequently, suggest a more complex mechanism of incorporation than that reported for thorium [17].

This point is confirmed from the XRD analysis which reveals the formation of several intermediates during the heating treatment. Indeed, while only the XRD lines of UO_2 are observed below 700 °C, that of the apatite structure appear at 800 °C (Fig. 1). From EPMA, the associated composition of this

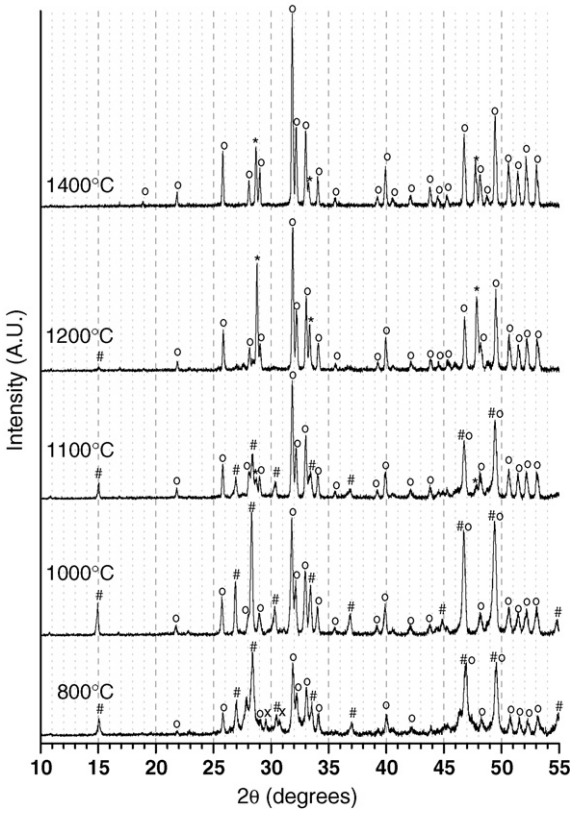

Fig. 1. Variation of the XRD patterns of (Nd, U)-britholite ($x = 0.5$) versus the heating temperature. Main XRD lines of apatite/britholite (o), Nd_2O_3 (x), $CaUO_4$ (#), and CaU_2O_{5+y} (*).

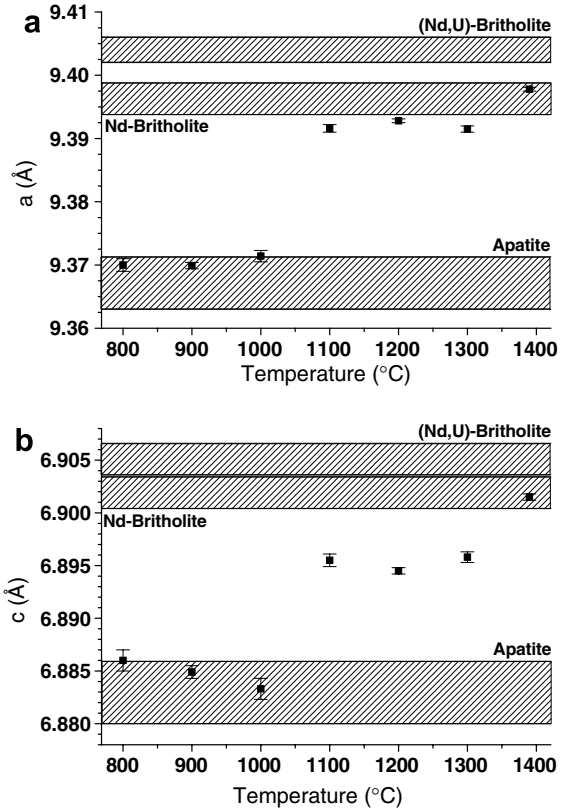

Fig. 2. Variations of refined unit cell parameters a (a) and c (b) for apatite or britholite phase versus the heating temperature ($t = 6$ h). The hatched zones correspond to the possible variations of the parameters of each phase according to the literature.

phase is close to that of $Ca_{10}(PO_4)_6F_2$ showing that neodymium and uranium are not incorporated in the structure at this temperature (Fig. 3) as it was already mentioned for thorium [17]. This point can be confirmed from the refined unit cell parameters associated to the apatite phase. Above 900 °C, they appear in good agreement with the values reported for $Ca_{10}(PO_4)_6F_2$ in the literature (Fig. 2), showing that silicate groups do not still participate to the structure. Moreover, the observation of the XRD lines of $CaUO_4$ (Fig. 1) indicates the oxidation of tetravalent uranium during the synthesis. This latter compound was already reported in literature when studying the $CaO–UO_2$ system [37]. It could result from the direct reaction between CaO (coming from the decomposition of $CaCO_3$) and UO_2. In this compound, uranium is present in the hexavalent oxidation state, leading to the characteristic yellow colour of the mixture

Table 1
Variation of the refined unit cell parameters of the apatite/britholite phase versus the heating temperature (expected formula $Ca_9Nd_{0.5}U_{0.5}(PO_4)_{4.5}(SiO_4)_{1.5}F_2$)

T (°C)	a (Å)	c (Å)	V (Å^3)	F_{20}	Assignment
800	9.370 (2)	6.8860 (15)	523.6 (4)	–	Apatite
900	9.370 (2)	6.8849 (15)	523.5 (4)	119 (0.0051; 33)	Apatite
1000	9.371 (2)	6.8833 (15)	523.5 (4)	66 (0.0084; 36)	Apatite
1100	9.392 (2)	6.8955 (15)	526.7 (4)	99 (0.0056; 36)	Britholite
1200	9.393 (2)	6.8945 (15)	526.8 (4)	168 (0.0033; 36)	Britholite
1300	9.392 (2)	6.8958 (15)	526.7 (4)	126 (0.0048; 36)	Britholite
1400	9.398 (2)	6.9015 (15)	527.9 (4)	195 (0.0031; 36)	Britholite

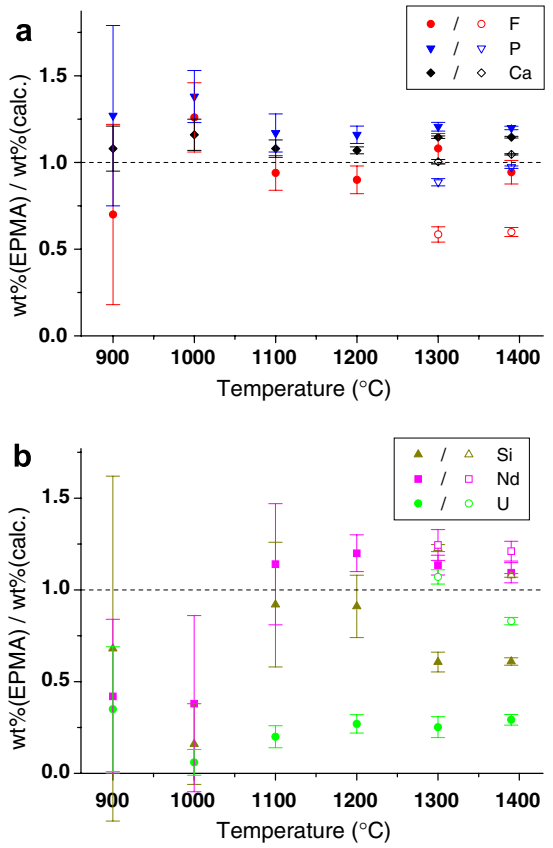

Fig. 3. Variations of the ratio between the experimental elementary weight percents (EPMA) and that expected for (Nd, U)-britholite ($x = 0.5$) versus the heating temperature ($t = 6$ h): F, P, Ca (a) and Si, Nd, U (b). Close symbols correspond to the major apatite/britholite phase and open symbols to the minor britholite composition.

already mentioned. Moreover, the associated characterization of the samples by μ-Raman indicates that it is in the hexapositive form, U^{6+}, and not as uranyl ion (absence of the strong vibration band associated to the ν_1 mode).

Between 900 and 1000 °C, the crystallinity of both $CaUO_4$ and apatite phases is significantly improved (as pointed by the decrease of the FWHM values of all the XRD lines). No additional compound is formed and EPMA results confirm that only small amounts of uranium, neodymium and silicon are incorporated in the apatite structure. Correlatively, the refined unit cell parameters remain consistent with that reported for $Ca_{10}(PO_4)_6F_2$ (Fig. 2).

Above 1100 °C, the XRD lines associated to $CaUO_4$ progressively disappear simultaneously to the observation of dark-green coloured compounds that crystallize with a fluorite-type structure like UO_2 ($a = 5.368(1)$ Å). Furthermore, the associated EPMA results allow to propose the formation of calcium uranate CaU_2O_{5+y}. This change in colour probably traduces the partial reduction of uranium(VI) into uranium(IV) at this temperature. Such reduction of actinide or lanthanide elements does not appear really surprising since it was already mentioned for uranium [38–40], plutonium or cerium [41,42] at high temperature. Indeed, in the case of tetravalent plutonium or cerium, both elements were found to be reduced to the trivalent oxidation state above 1000 °C leading to the formation of $PuPO_4$ or $CePO_4$ monazites [41,42]. Moreover, for uranium, the preparation of $U(UO_2)(PO_4)_2$ from $UClPO_4 \cdot 4H_2O$ through a complex redox mechanism was already described when heating in air. In this study, uranium(IV) was first oxidized into uranium(VI) in air up to 600 °C then partly reduced between 600 and 800 °C, leading to a mole ratio U(VI)/U(IV) equal to 1, characteristic of the final $U(UO_2)(PO_4)_2$ compound [40]. The same kind of reaction could be responsible of the existence of both uranium(IV) and uranium(VI) in the CaU_2O_{5+y} phase.

The XRD lines of $CaUO_4$ fully disappear at 1200 °C on behalf of that of CaU_2O_{5+y} (Fig. 1). The variation of the unit cell parameters seems to indicate that neodymium and silicon are progressively incorporated in the apatite structure to form the britholite phase. However, this temperature appears higher than that reported for thorium (i.e. 1000 °C). This temperature shift could result from the formation of the intermediate $CaUO_4$ as a stabilized phase. Consequently, it appears necessary to perform the heating treatment of the mixture above 1200 °C to proceed to the complete decomposition of $CaUO_4$ thus to reach the significant incorporation of uranium in the britholite structure.

The CaU_2O_{5+y} phase is still present in the mixture above 1300 °C even though all the relative intensities of the associated XRD lines decrease significantly compared to that of the britholite structure. At 1400 °C, the system is clearly polyphase. It is composed by CaU_2O_{5+y} (white grains in the SEM micrographs reported in Fig. 4 and in the X-EDS mapping given in Fig. 5) and by (Nd, U)-britholite (hexagonal grains of 10–30 μm in length: Figs. 4(a) and 5) in which either uranium and silicate are incorporated, as indicated by the small increase of the unit cell parameters (Fig. 2). Moreover, from EPMA results, uranium is not homogeneously distributed in the britholite phase: two compositions being evidenced as it is clearly observed in several micrographs (e.g.

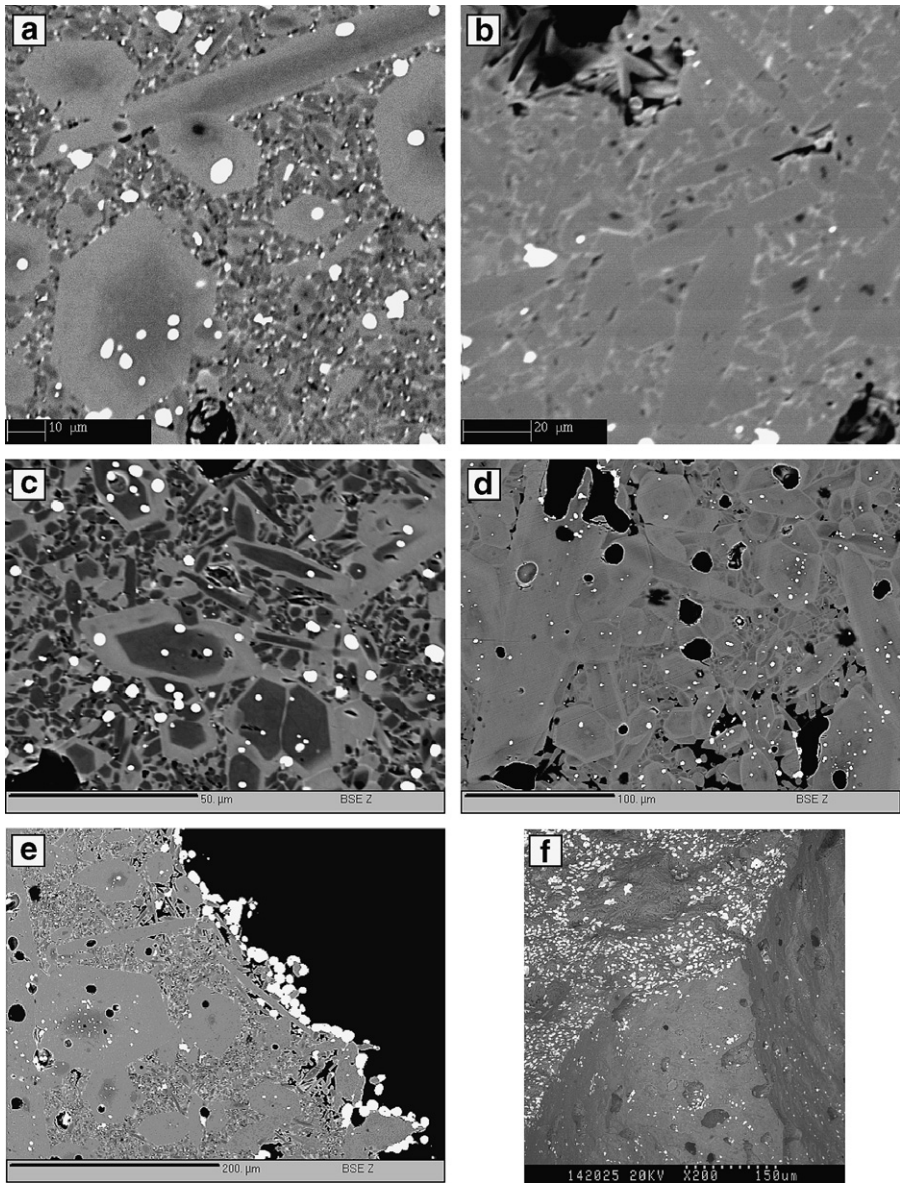

Fig. 4. SEM observations of (Nd, U)-britholite ($x = 0.5$) using a mechanical grinding (30 Hz/15 min) for several conditions of synthesis: 6 h at 1400 °C (a) and (c); compaction/6 h at 1400 °C (b), (e) and (f) and 12 h at 1400 °C (d).

Fig. 4(c)) recorded in the BSE mode which underlines the differences of composition especially for heavy elements. The first one (observed in light grey in Fig. 4(c)) is mainly uranium enriched (8.5 wt% instead of 10.3 wt% expected). It appears as a minor phase and surrounds the second phase (dark grey, low incorporation rate of uranium close to 3.0 wt%), which corresponds to the major composition of britholite. It is worth to note that for both compositions, the mole ratio $(PO_4 + SiO_4)/(Ca + Nd + U)$ is in good agreement with the britholite stoichiometry (near to 0.58 for an expected value of 0.6). The average composition proposed for this uranium depleted phase is thus $Ca_{9.61}Nd_{0.52}U_{0.14}(PO_4)_{5.15}(SiO_4)_{0.88}F_{1.80}O_{0.47}$ while the uranium enriched exhibits the following average composition: $Ca_{9.44}Nd_{0.60}U_{0.42}(PO_4)_{4.40}(SiO_4)_{1.65}F_{1.20}O_{0.68}$. While both (Nd, U)-britholites compositions are always observed, their relative proportions significantly depend on the conditions of preparation.

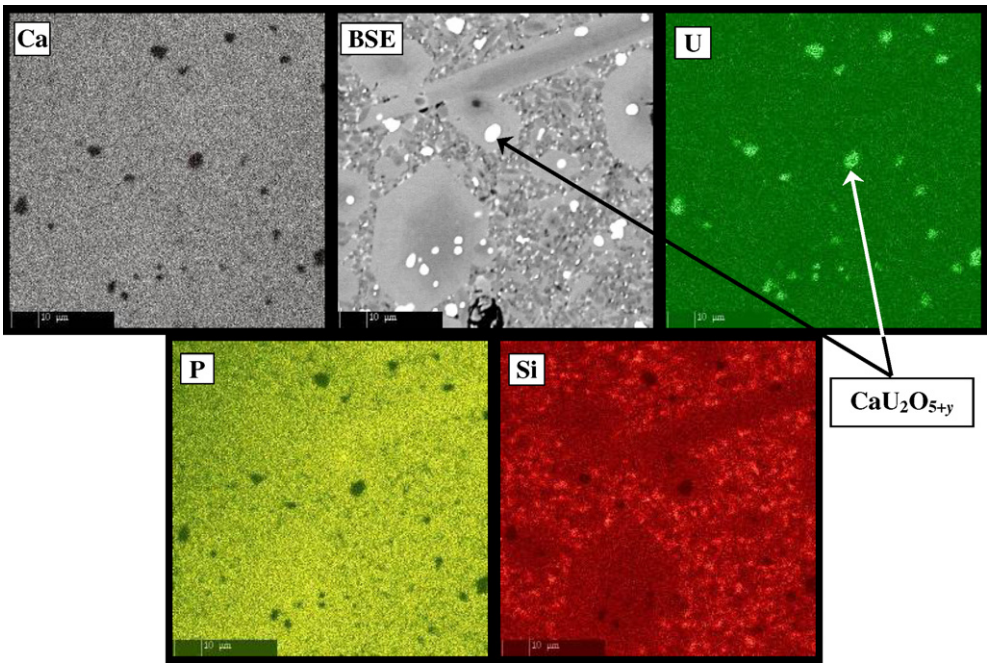

Fig. 5. X-EDS mapping recorded for (Nd, U)-britholite prepared through initial mechanical grinding (30 Hz/15 min) then heating at 1400 °C for 6 h.

3.1.2. Characterization by μ-Raman and IR spectroscopies

All the samples prepared after heating at 1400 °C were also characterized through μ-Raman and IR spectroscopies (Fig. 6). As described in Fig. 6, all the vibration bands corresponding to phosphate and silicate tetrahedra are observed and a global assignment is proposed on the basis of that reported in literature for $La_{1-2x}Ca_xAn^{IV}_x(PO_4)$ [43], β-TPD and associated β-TUPD solid solutions [8,44], $Ca_xLa_y(SiO_4)_{6-u}(PO_4)_uO_t$ (with $0 \leqslant u \leqslant 6$) [45], $Ca_3(PO_4)_2$ [45], $ThSiO_4$ [46] and $ZrSiO_4$ [47]. As a summary, the vibration bands located at 430 and 450 cm^{-1} (μ-Raman), near to 520 cm^{-1} (IR) and between 560 and 610 cm^{-1} (IR and μ-Raman) can be assigned to the doubly degenerate symmetric bending modes δ_s(P–O) and δ_s(Si–O) and to the triply degenerate antisymmetric bending modes δ_{as}(Si–O) and δ_{as}(P–O), respectively. In the domain usually associated to the stretching modes, the vibrations bands observed between 840 and 890 cm^{-1} (IR and μ-Raman) and near to 910 cm^{-1} (μ-Raman) can be associated to the symmetric ν_S(Si–O) and antisymmetric ν_{as}(Si–O) stretching modes of silicate groups, respectively. For phosphate groups, they are observed near to 960 cm^{-1} (μ-Raman: strong and narrow band corresponding to ν_s(P–O) and characteristic of the apatite structure) and between 1000 and 1100 cm^{-1} (IR and μ-Raman: ν_{as}(P–O)), respectively. Finally the vibration band located at 690 cm^{-1} can be associated to some stretching modes of U–O edge, as already described in literature for tetravalent actinide hydroxide phosphates $M(OH)PO_4$ and diactinide oxide phosphates $M_2O(PO_4)_2$ [48]. Moreover, it is worth to note the absence of the strong and narrow vibration band near to 870 cm^{-1}, characteristic of the ν_1 symmetric stretching mode of the uranyl (UO_2^{2+}) units [49–51] which confirms that hexavalent uranium is present as U^{6+} in CaU_2O_{5+y} phase (this point was also checked in pure calcium uranate samples, as already mentioned).

3.1.3. Specific study of the $CaO–UO_2$ system

In order to underline the redox processes occurring during the heating treatment, the $CaO–UO_2$ system was particularly examined, especially pointing out the relationship between both $CaUO_4$ and CaU_2O_{5+y} compounds. It was clearly shown that $CaUO_4$ begins to decompose into CaU_2O_{5+y} above 1000 °C, which is consistent with the data reported in literature even though Pialoux and Touzelin reported an higher temperature for the decomposition of $CaUO_4$ (i.e. 1200 °C) probably due to the

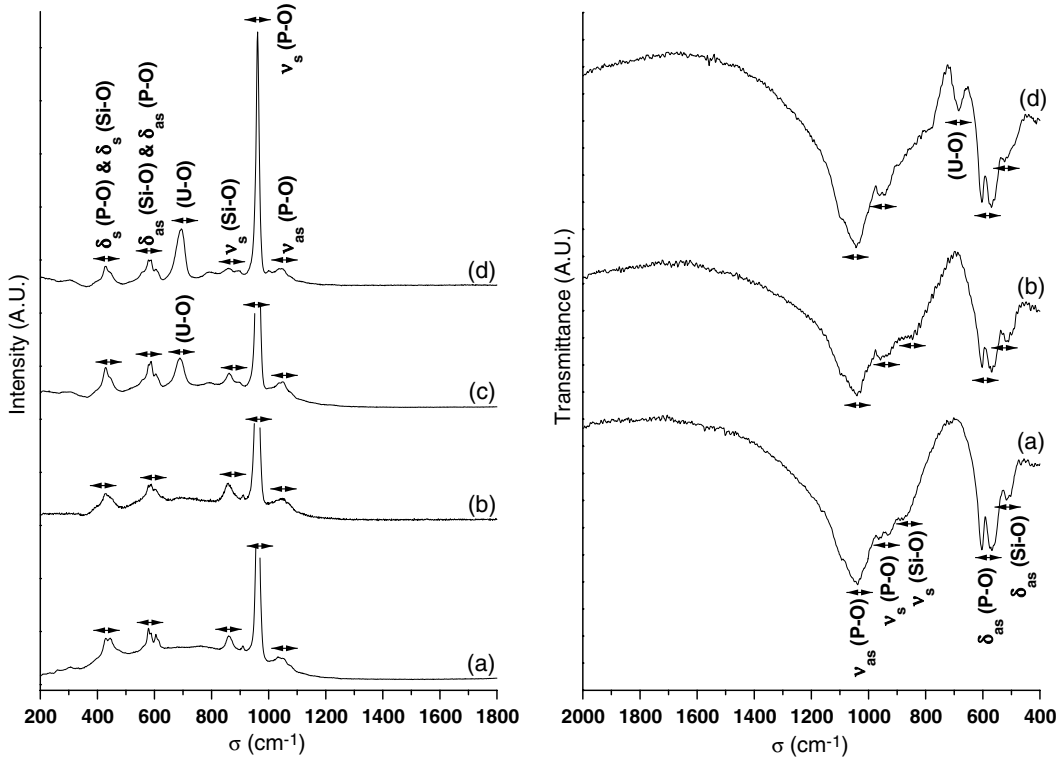

Fig. 6. μ-Raman (left) and infrared (right) spectra of Nd-britholite (a), (Nd, Th)-britholite ($x = 0.5$) (b), and (Nd, U)-britholites for $x = 0.25$ (c) and $x = 0.5$ (d).

lower reactivity of the initial powders used in their study [37]. These authors finally formed the $U_{1-\delta}Ca_{\delta}O_{2-\delta}$ solid solution above 1400 °C. In our conditions, the progressive reduction of tetravalent uranium, associated to this decomposition, can be clearly correlated to the progressive incorporation of tetravalent uranium in the britholite structure through diffusion processes. This latter point was confirmed by extending the heating time at 1400 °C from 6 to 12 h (Fig. 4(c) and (d)) which main consequence is the significant reduction of the amount of calcium uranate CaU_2O_{5+y} in the mixture.

In order to limit the formation of $CaUO_4$ then CaU_2O_{5+y} as secondary phases, the conditions of synthesis were optimized (see following sections) especially by varying the uranium reagent, the grinding conditions (in order to modify the initial reactivity) or by making the compaction of the initial powdered mixture. Finally, because thorium is characterized by the unique stabilized tetravalent oxidation state, the simultaneous incorporation of thorium and uranium was finally examined.

3.2. Incorporation of uranium versus the uranium weight loading

As mentioned when studying the preparation of (Nd, Th)-britholites [17], the incorporation of uranium should be increased significantly when improving the efficiency of the grinding step (optimized retained conditions: 15 min and 30 Hz of oscillation frequency: see next section). Such conditions of preparation were considered for several uranium weight loadings in (Nd, U)-britholites $Ca_9Nd_{1-x}U_x(PO_4)_{5-x}(SiO_4)_{1+x}F_2$ ranging from $x = 0$ to $x = 1$.

The results of EPMA experiments performed on (Nd, U)-britholite samples are reported in Table 2. The associated XRD patterns are given in Fig. 7 and the associated refined unit cell parameters are gathered in Table 3. For all the samples, the unit cell parameters slightly decrease compared to that reported for Nd-britholite which traduces some compensation due to the simultaneous replacement of trivalent neodymium by the smaller tetravalent uranium ($^{VII}r^{3+}_{Nd} = 1.05$ Å and $^{VII}r^{4+}_{U} = 0.95$ Å [52]) and of phosphate groups by the bigger silicate entities.

Table 2
Results of EPMA analysis of $Ca_9Nd_{1-x}U_x(PO_4)_{5-x}(SiO_4)_{1+x}F_2$ britholites for $0.25 \leqslant x \leqslant 1$ (mechanical grinding : 15 min, 30 Hz)

	$x = 0.25$		$x = 0.5$		$x = 0.75$			$x = 1$	
	Calc.	Exp.	Calc.	Exp.	Calc.	Exp. (phase I)	Exp. (phase II)	Calc.	Exp.
wt% (O)	33.9	34.4 ± 0.2	33.2	34.2 ± 0.3	32.6	34.8 ± 0.2	35.8 ± 0.2	32.0	35.4 ± 0.2
wt% (F)	3.4	2.1 ± 0.2	3.3	1.7 ± 0.2	3.2	1.9 ± 0.1	3.0 ± 0.2	3.2	2.0 ± 0.3
wt% (Si)	3.1	3.1 ± 0.1	3.7	3.6 ± 0.1	4.2	3.3 ± 0.1	1.8 ± 0.1	4.7	3.4 ± 0.6
wt% (P)	13.0	13.4 ± 0.2	12.1	12.6 ± 0.2	11.2	13.3 ± 0.1	15.9 ± 0.3	10.3	13.7 ± 0.7
wt% (Ca)*	31.9	32.4 ± 0.4	31.2	32.4 ± 0.2	30.6	33.9 ± 0.1	37.0 ± 0.4	30.0	35.8 ± 0.6
wt% (Nd)	9.5	9.8 ± 0.6	6.2	7.0 ± 0.3	3.1	3.8 ± 0.3	3.0 ± 0.3	–	–
wt% (U)	5.2	4.8 ± 0.2	10.3	8.5 ± 0.2	15.1	9.0 ± 0.1	3.6 ± 0.5	19.8	9.6 ± 1.2
Mole ratios									
Si/P	0.263	0.254 ± 0.010	0.333	0.316 ± 0.008	0.412	0.273 ± 0.005	0.122 ± 0.011	0.500	0.275 ± 0.063
Nd/Ca	0.083	0.084 ± 0.006	0.056	0.060 ± 0.002	0.028	0.031 ± 0.002	0.023 ± 0.002	–	–
U/Ca	0.028	0.025 ± 0.001	0.056	0.044 ± 0.001	0.083	0.044 ± 0.003	0.016 ± 0.003	0.111	0.046 ± 0.006
(Si + P)/(Ca + Nd + U)	0.600	0.607 ± 0.005	0.600	0.599 ± 0.003	0.600	0.602 ± 0.003	0.601 ± 0.004	0.600	0.604 ± 0.006
Proposed formulae									
Ca*	9	9.02 ± 0.11	9	9.05 ± 0.06	9	9.53 ± 0.03	9.86 ± 0.11	9	9.81 ± 0.16
Nd	0.75	0.76 ± 0.05	0.5	0.54 ± 0.02	0.25	0.30 ± 0.02	0.22 ± 0.02	0	0
U	0.25	0.22 ± 0.01	0.5	0.40 ± 0.01	0.75	0.42 ± 0.01	0.16 ± 0.02	1	0.44 ± 0.06
PO_4	4.75	4.84 ± 0.07	4.5	4.55 ± 0.07	4.25	4.84 ± 0.04	5.49 ± 0.10	4	4.87 ± 0.25
SiO_4	1.25	1.23 ± 0.04	1.5	1.44 ± 0.04	1.75	1.32 ± 0.04	0.67 ± 0.04	2	1.33 ± 0.23
F	2	1.22 ± 0.12	2	1.01 ± 0.12	2	1.10 ± 0.06	1.67 ± 0.11	2	1.16 ± 0.17
O	0	0.27 ± 0.01	0	0.45 ± 0.01	0	0.37 ± 0.01	0.10 ± 0.01	0	0.15 ± 0.01

* Overestimation of the calcium amount during the EPMA analyses due to simultaneous presence of calcium and uranium (this phenomenon was also observed when studying $Ca_{0.5}Th_{0.5-x}U_x(PO_4)$ brabantites).

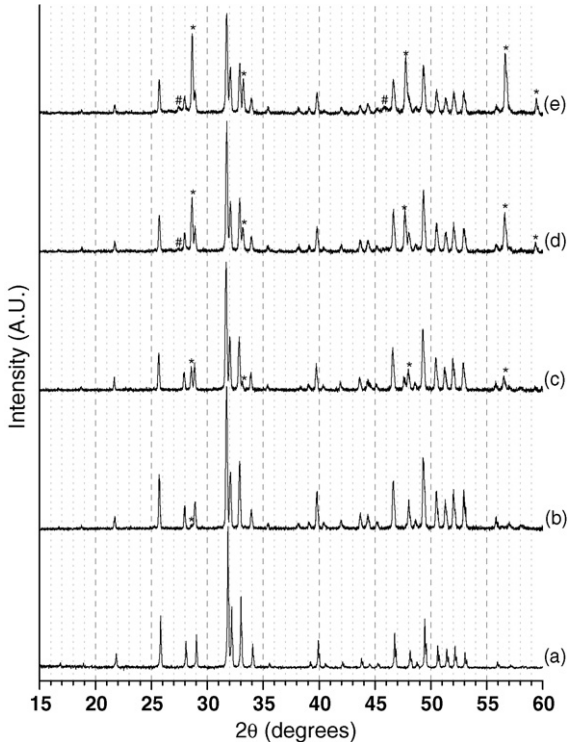

Fig. 7. XRD patterns of (Nd, U)-britholites of formula $Ca_9Nd_{1-x}U_x(PO_4)_{5-x}(SiO_4)_{1+x}F_2$ with $x = 0$ (a), 0.25 (b), 0.5 (c), 0.75 (d) and 1 (e). Main XRD lines of CaU_2O_{5+y} (*) and of $Ca_3(Si_3O_9)$ (#).

For the $Ca_9Nd_{0.75}U_{0.25}(PO_4)_{4.75}(SiO_4)_{1.25}F_2$ composition, the XRD lines associated to CaU_2O_{5+y} are very weak which traduces the quantitative incorporation of uranium in the britholite phase. This point is also confirmed from EPMA experiments (Table 2) that lead to an experimental uranium weight loading of 4.8 ± 0.2 wt% (instead of 5.2 wt% expected). The increase of the uranium weight loading significantly degrades the homogeneity of (Nd, U)-britholites. Indeed, the more important is the uranium weight loading, the more intense are the XRD lines of CaU_2O_{5+y} while the difference between both expected and experimental uranium weight percents increases (Fig. 7). This observation can be also correlated to the appearance of the XRD lines of the pseudowollastonite, $Ca_3(SiO_3)_9$, as the host phase for the silicon excess resulting from the incomplete incorporation of tetravalent uranium in the britholite structure. While the uranium incorporation in (Nd, U)-britholites appears rather satisfying for $x < 0.5$, a limit of uranium weight loading of 9–9.6 wt% is observed for $x \geqslant 0.5$. Consequently, the x value reached only about 0.45 (Table 2). Such a limit of uranium incorporation is plotted in Fig. 8 for two different conditions of initial mechanical grindings underlining the interest of the mechanical grinding step prior to perform the heating treatment at 1400 °C (see next section). As already mentioned, such a limit of uranium incorporation in the britholite structure was already described (but not explained) by El Ouenzerfi et al. [34] in the field of the preparation of $Ca_aLa_bU_x(PO_4)_3(SiO_4)_3O_c$

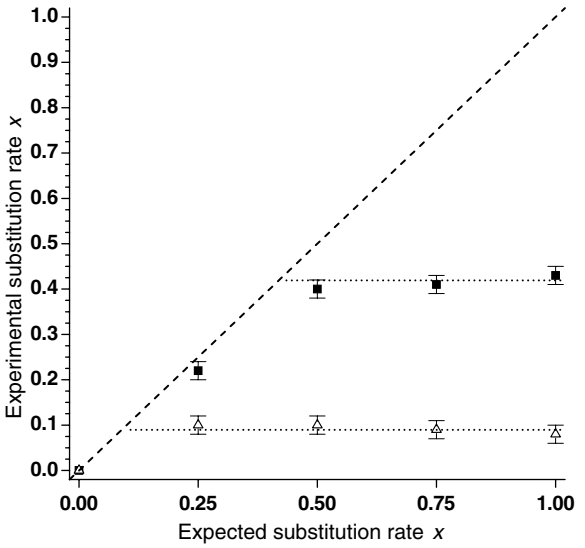

Fig. 8. Variation of the experimental incorporation rate of uranium versus that expected for 15 Hz/15 min (Δ) and 30 Hz/15 min (■) grinding conditions. Maximum incorporation rate for both conditions (dot lines) and expected variation (dash line).

Table 3
Refined unit cell parameters of $Ca_9Nd_{1-x}U_x(PO_4)_{5-x}(SiO_4)_{1+x}F_2$ britholites ($0 \leqslant x \leqslant 1$)

$x_{expected}$	Composition*	a (Å)	c (Å)	V (Å^3)	F_{20}
0	$Ca_{9.11}Nd_{1.02}(PO_4)_{5.15}(SiO_4)_{1.00}F_{0.35}O_{0.73}$	9.402 (2)	6.9022 (15)	528.4 (4)	148 (0.0041; 33)
0.25	$Ca_{9.02}Nd_{0.76}U_{0.22}(PO_4)_{4.84}(SiO_4)_{1.23}F_{1.22}O_{0.27}$	9.399 (2)	6.8959 (15)	527.5 (4)	170 (0.0038; 31)
0.50	$Ca_{9.05}Nd_{0.54}U_{0.40}(PO_4)_{4.55}(SiO_4)_{1.44}F_{1.01}O_{0.45}$	9.397 (2)	6.8973 (15)	527.5 (4)	128 (0.0039; 40)
0.75	$Ca_{9.30}Nd_{0.29}U_{0.41}(PO_4)_{4.73}(SiO_4)_{1.29}F_{1.07}O_{0.35}$	9.392 (2)	6.8948 (15)	526.7 (4)	173 (0.0035; 33)
1	$Ca_{9.56}U_{0.43}(PO_4)_{4.74}(SiO_4)_{1.29}F_{1.13}O_{0.17}$	9.383 (2)	6.8898 (15)	525.4 (4)	198 (0.0028; 36)

* Composition of the major britholite phase determined from EPMA experiments.

samples (with $a + b + x = 10$, a and b near to 5 and $0 \leqslant x \leqslant 0.8$). For $x > 0.8$, the system was always composed by the britholite phase, UO_2 and U_3O_8 [34].

3.3. Optimization of the conditions of synthesis in the field of a better incorporation of uranium in britholites

3.3.1. Effect of the initial uranium reagent

In order to improve the incorporation of uranium in the britholite structure, complementary experiments were developed by substituting uranium dioxide by several uranium phosphates (such as uranium diphosphate, α-UP_2O_7, or uranium phosphate hydrogenphosphate hydrate, $U_2(PO_4)_2(HPO_4) \cdot H_2O$) as initial reagents. The interest of this kind of synthesis mainly results in the modification of the initial reactivity of the powders used and in the attempt to avoid the formation of calcium uranate through the use of more stable and less reactive uranium phosphate phases. Both XRD analysis and EPMA experiments reveal that the uranium incorporation is significantly improved when using UPHPH as the initial reagent, due to a higher specific surface area (8–12 $m^2\ g^{-1}$) compared to that of α-UP_2O_7 (0.3 $m^2\ g^{-1}$) or of UO_2 (1.5–2.3 $m^2\ g^{-1}$). Consequently, the uranium weight percentage in the resulting powder reaches up to 9.3 wt% in the uranium enriched britholite from UPHPH instead of 8.9 and 8.2 wt% when using UO_2 and α-UP_2O_7, respectively. However, all the results obtained allow to conclude that even though it is possible to reduce significantly the proportion of calcium uranate CaU_2O_{5+y} in the final sample, it is not possible to guarantee its complete elimination.

3.3.2. Effect of the grinding conditions

As the reactivity of the initial mixture appears as a key parameter driving the incorporation of uranium in the britholite structure, the second parameter studied to increase the uranium weight loading in the prepared samples was the initial homogenization of the mixture. For this reason, some manual and mechanical grinding steps with various conditions (steps of 15 min at 15 or 30 Hz) were developed prior to perform the final heating treatment at 1400 °C for 6 h under inert atmosphere, as already described.

In all the samples, the analysis of the XRD patterns of the fired powders (Fig. 9, $x = 0.5$) revealed the formation of a polyphase system composed by

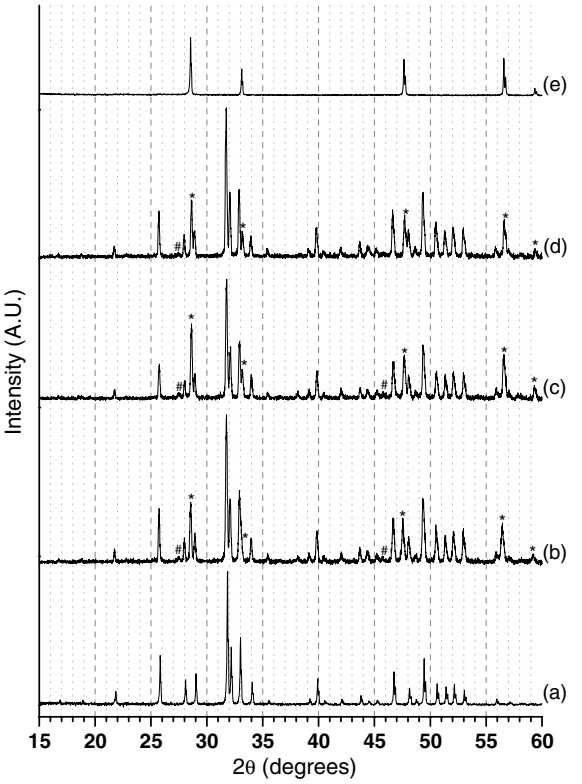

Fig. 9. XRD patterns of Nd-britholite (a), and (Nd, U)-britholite prepared through manual grinding (b), mechanical grinding (15 Hz/15 min) (c) and mechanical grinding (30 Hz/15 min) (d). XRD pattern of CaU_2O_{5+y} (e). Main XRD lines of CaU_2O_{5+y} (*) and of $Ca_3(Si_3O_9)$ (#).

(Nd, U)-britholite (as the major phase) and of significant amounts of CaU_2O_{5+y}. It is worth to note that very small amounts of the pseudowollastonite, $Ca_3(SiO_3)_9$, are also detected in some samples confirming the role of this host phase for the silicon excess consequently to the incomplete incorporation of tetravalent uranium in the britholite structure. These results also suggest that the complete incorporation of uranium is difficult to reach even when using an efficient initial homogenization step.

The associated EPMA results (Table 4) confirmed the formation of two compositions of (Nd, U)-britholite for manually ground samples, as already described in the previous sections with a major britholite phase containing only 3.5 wt% of uranium. As already mentioned for (Nd, Th)-britholites [17], the use of a grinding step allows to improve significantly the homogeneity of the samples (only one britholite composition is evidenced for all the ground samples; Table 4) and to increase

Table 4
Results of EPMA analysis of (Nd, U)-britholites ($x = 0.5$) versus the grinding conditions and the calcination form: powder or pellet

	Calc.	Calcination in the powder form				Pellet**
		Manual grinding		Mechanical grinding		
		Phase I (maj.)	Phase II (min.)	15 Hz – 15 min.	30 Hz – 15 min.	
wt% (O)	33.2	35.7 ± 0.1	33.9 ± 0.2	35.7 ± 0.3	36.5 ± 0.2	34.3 ± 0.4
wt% (F)	3.3	3.1 ± 0.1	2.1 ± 0.1	3.2 ± 0.2	0.2 ± 0.1	2.3 ± 0.2
wt% (Si)	3.7	2.0 ± 0.1	3.6 ± 0.2	2.1 ± 0.3	3.0 ± 0.1	3.5 ± 0.3
wt% (P)	12.1	15.0 ± 0.1	12.0 ± 0.2	15.1 ± 0.4	13.9 ± 0.3	12.7 ± 0.3
wt% (Ca)*	31.2	34.7 ± 0.2	31.6 ± 0.1	34.5 ± 0.4	32.9 ± 0.3	32.4 ± 0.4
wt% (Nd)	6.2	6.0 ± 0.3	7.9 ± 0.3	7.1 ± 0.3	7.6 ± 0.3	6.8 ± 0.4
wt% (U)	10.3	3.5 ± 0.2	8.9 ± 0.4	2.3 ± 0.3	5.9 ± 0.5	8.0 ± 0.4
Mole ratio						
Si/P	0.333	0.148 ± 0.002	0.330 ± 0.026	0.152 ± 0.030	0.241 ± 0.016	0.302 ± 0.019
Nd/Ca	0.056	0.048 ± 0.002	0.070 ± 0.002	0.057 ± 0.002	0.064 ± 0.003	0.058 ± 0.004
U/Ca	0.056	0.017 ± 0.001	0.048 ± 0.002	0.011 ± 0.002	0.030 ± 0.003	0.042 ± 0.003
(Si + P)/(Ca + Nd + U)	0.600	0.602 ± 0.001	0.587 ± 0.001	0.609 ± 0.008	0.617 ± 0.004	0.604 ± 0.013
Expected formula				*Proposed formulae*		
Ca*	9.0	9.40 ± 0.05	9.13 ± 0.03	9.31 ± 0.11	9.21 ± 0.08	9.19 ± 0.09
Nd	0.5	0.45 ± 0.02	0.64 ± 0.02	0.53 ± 0.02	0.59 ± 0.02	0.54 ± 0.03
U	0.5	0.16 ± 0.05	0.44 ± 0.02	0.10 ± 0.01	0.27 ± 0.02	0.38 ± 0.02
PO_4	4.5	5.25 ± 0.07	4.50 ± 0.08	5.26 ± 0.14	5.02 ± 0.11	4.70 ± 0.10
SiO_4	1.5	0.78 ± 0.04	1.48 ± 0.07	0.80 ± 0.11	1.21 ± 0.04	1.41 ± 0.08
F	2.0	1.77 ± 0.06	1.30 ± 0.06	1.84 ± 0.12	0.12 ± 0.06	1.32 ± 0.08
O	0	0.08 ± 0.01	0.61 ± 0.01	–	0.63 ± 0.01	0.24 ± 0.01

* Overestimation of the calcium amount during the EPMA analyses due to simultaneous presence of calcium and uranium (this phenomenon was also observed when studying $Ca_{0.5}Th_{0.5-x}U_x(PO_4)$ brabantites).
** Average values obtained from EPMA results obtained on three sintered samples.

significantly the incorporation of uranium when using a grinding step at 30 Hz (5.9 wt% (U)) instead of 15 Hz (2.3 wt% (U)). However, it remains insufficient to guarantee the complete elimination of CaU_2O_{5+y}.

3.3.3. Effect of the compaction of the initial powdered mixture

The previous results showed that the efficient homogenization and increase of reactivity through grinding steps are not sufficient to ensure the quantitative incorporation of uranium in the (Nd, U)-britholite structure, probably due to the formation of $CaUO_4$ as a main chemical intermediate by the way of the oxidation of uranium(IV) into uranium(VI). Some attempts to avoid such an oxidation were also performed through the compaction of the initial mixture (100–200 MPa) after a mechanical grinding step (30 Hz, 15 min) and before performing the heating treatment at 1400 °C. EPMA results (Table 4) confirm the better uranium incorporation in the (Nd, U)-britholite phase (between 7.4 and 8.5 wt% (U)) than that obtained for powdered samples (typically close to 5–6 wt% (U)). All the elementary weight percents and mole ratios are consistent with that expected. Moreover, the associated refined cell parameters, obtained from grazing XRD, i.e. $a = 9.404(2)$ Å and $c = 6.9051(15)$ Å ($V = 528.8(4)$ Å^3) are in good agreement with that expected on the basis of the results obtained for (Nd, Th)-britholites or (Nd, Th, U)-britholites (see next section) and of the uranium weight loading. Finally, the SEM observations in the BSE mode show an improved homogeneity in the bulk material (Fig. 4(b)) compared to that noted for powdered samples (Fig. 4(a)). Indeed, the formation of calcium uranate is mainly located at the surface of the (Nd, U)-britholite samples and inside the open porosity (Fig. 4(e) and 4(f)) which strongly underlines the essential role of the solid/gas interface on the formation of CaU_2O_{5+y} during the heating treatment, even in inert conditions. The localization of the calcium uranate phase was also checked from grazing XRD on raw and polished samples. Indeed, while the XRD lines of CaU_2O_{5+y} are predominant for the raw sample, they strongly decrease after the polishing step.

3.3.4. Effect of the simultaneous incorporation of thorium and uranium

As it was already discussed, the quantitative incorporation of thorium in synthetic (Nd, Th)-britholites can be successfully reached from several thorium reagents after heating at 1400 °C [17]. On the contrary that of uranium is limited probably due to the formation of $CaUO_4$ then CaU_2O_{5+y} as intermediate phases. In order to avoid (or limit) the formation of such compounds during the heating treatment, the simultaneous incorporation of tetravalent thorium and uranium in (Nd, Th, U)-britholites, i.e. $Ca_9Nd_{0.5}Th_{0.5-z}U_z(PO_4)_{4.5}(SiO_4)_{1.5}F_2$, was developed from several thorium–uranium(IV) dioxide solid solutions $Th_{1-w}U_wO_2$ (with $w = 0.11$, 0.25, 0.50 and 0.67), as initial reagents. These actinide dioxide solid solutions were prepared by precipitation of oxalates $Th_{1-w}U_w(C_2O_4)_2 \cdot 2H_2O$ then heating at 800 °C for 10 h in Ar/H_2 atmosphere (S_{BET} of the resulting powder between 6.0 and 8.0 $m^2\,g^{-1}$). All the other conditions of preparation of (Nd, Th, U)-britholites were kept to the optimized values already discussed (mechanical grinding of the initial mixture for 15 min at 30 Hz, heating treatment at 1400 °C for 6 h).

The results of EPMA experiments obtained for the prepared (Nd, Th, U)-britholites samples are gathered in Table 5 while the associated XRD patterns are reported in Fig. 10. All these experiments confirmed the significant improvement of the samples homogeneity. Indeed, only one composition of (Nd, Th, U)-britholite is observed for each sample prepared. One the basis of the results reported in Table 5, thorium and uranium are quantitatively incorporated in the (Nd, Th, U)-britholite structure and the amount of calcium uranate CaU_2O_{5+y} is significantly reduced which is confirmed from XRD (Fig. 10). Indeed, XRD patterns of both compounds with smaller uranium weight loadings (corresponding to $z = 0.055$ and 0.125) do not reveal any XRD lines of CaU_2O_{5+y} while they appear with very low intensities for uranium enriched compositions (i.e. $z = 0.25$ and 0.335). As a confirmation of the simultaneous incorporation of both tetravalent actinides, the unit cell parameters of (Nd, Th, U)-britholite samples were refined (Table 6). Their variations versus the average substitution rate of thorium by tetravalent uranium are plotted in Fig. 11. Both a and c unit cell parameters decrease linearly when thorium is progressively substituted by uranium(IV) in the structure. This observation appears in good agreement with the replacement of thorium ($^{VII}r^{4+}_{Th} = 1.00$ Å [52]) by the smaller uranium ($^{VII}r^{4+}_{U} = 0.95$ Å [52]) when

Table 5
Results of EPMA analysis of $Ca_9Nd_{0.5}Th_{0.5-z}U_z(PO_4)_{4.5}(SiO_4)_{1.5}F_2$ britholites for $0 < z < 0.5$

	$z = 0.055$		$z = 0.125$		$z = 0.25$		$z = 0.335$	
	Calc.	Exp.	Calc.	Exp.	Calc.	Exp.	Calc.	Exp.
wt% (O)	33.2	34.1 ± 0.2	33.2	34.0 ± 0.1	33.2	34.0 ± 0.2	33.4	34.0 ± 0.7
wt% (F)	3.3	1.6 ± 0.2	3.3	1.7 ± 0.1	3.3	1.6 ± 0.1	3.3	1.7 ± 0.1
wt% (Si)	3.7	3.5 ± 0.2	3.7	3.5 ± 0.2	3.7	3.8 ± 0.1	3.6	3.8 ± 0.2
wt% (P)	12.1	12.6 ± 0.1	12.1	12.6 ± 0.2	12.1	12.2 ± 0.1	12.1	12.3 ± 0.3
wt% (Ca)	31.3	31.4 ± 0.2	31.3	31.6 ± 0.2	31.3	31.9 ± 0.3	31.2	32.1 ± 0.4
wt% (Nd)	6.3	6.4 ± 0.3	6.3	6.6 ± 0.4	6.3	6.4 ± 0.2	6.3	6.3 ± 0.3
wt% (Th)	9.0	9.2 ± 0.2	7.5	7.5 ± 0.2	5.0	4.7 ± 0.3	3.3	3.5 ± 0.1
wt% (U)	1.1	1.1 ± 0.1	2.6	2.3 ± 0.1	5.2	5.3 ± 0.2	6.9	6.4 ± 0.2
Mole ratio								
Si/P	0.333	0.309 ± 0.021	0.333	0.306 ± 0.017	0.333	0.346 ± 0.011	0.333	0.338 ± 0.009
U/Th	0.124	0.122 ± 0.008	0.333	0.29 ± 0.01	1.00	1.10 ± 0.07	2.03	1.77 ± 0.09
(Nd + Th + U)/Ca	0.111	0.113 ± 0.004	0.111	0.113 ± 0.005	0.111	0.110 ± 0.003	0.111	0.107 ± 0.003
(Si + P)/(Ca + Nd + Th + U)	0.600	0.612 ± 0.005	0.600	0.606 ± 0.006	0.600	0.603 ± 0.004	0.600	0.60 ± 0.01
Proposed formulae								
Ca	9	8.98 ± 0.06	9	8.98 ± 0.06	9	9.01 ± 0.08	9	9.03 ± 0.11
Nd	0.5	0.51 ± 0.02	0.5	0.53 ± 0.03	0.5	0.50 ± 0.02	0.5	0.49 ± 0.02
Th	0.445	0.45 ± 0.01	0.375	0.38 ± 0.01	0.25	0.23 ± 0.01	0.165	0.17 ± 0.01
U	0.055	0.05 ± 0.01	0.125	0.11 ± 0.01	0.25	0.25 ± 0.01	0.335	0.30 ± 0.01
PO_4	4.5	4.67 ± 0.04	4.5	4.64 ± 0.07	4.5	4.48 ± 0.04	4.5	4.48 ± 0.11
SiO_4	1.5	1.44 ± 0.08	1.5	1.42 ± 0.08	1.5	1.55 ± 0.04	1.5	1.51 ± 0.08
F	2	0.96 ± 0.12	2	1.00 ± 0.06	2	0.95 ± 0.06	2	0.99 ± 0.06
O	0	0.38 ± 0.01	0	0.46 ± 0.01	0	0.43 ± 0.01	0	0.47 ± 0.01

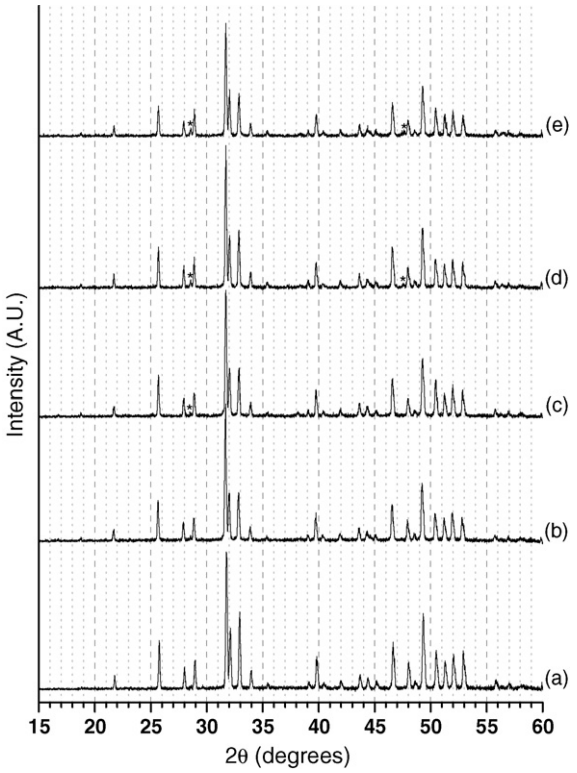

Fig. 10. Variations of the XRD patterns for (Nd, Th, U)-britholites with $z = 0$ (a), $z = 0.055$ (b), $z = 0.125$ (c), $z = 0.250$ (d) and $z = 0.335$ (e). Main XRD lines of CaU_2O_{5+y} (*).

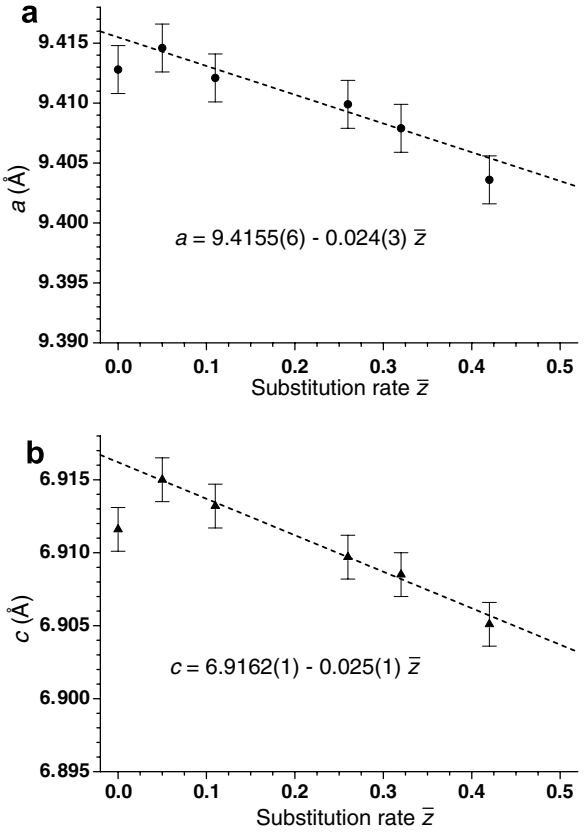

Fig. 11. Variations of refined unit cell parameters a (a) and c (b) of $Ca_9Nd_{0.5}Th_{0.5-z}U_z(PO_4)_{4.5}(SiO_4)_{1.5}F_2$ britholites versus the average substitution rate $\bar{z}$.

keeping constant the mole ratio SiO_4/PO_4 (i.e. 0.33). From these linear variations, it is thus possible to determine the unit cell values corresponding to the full substitution of thorium by uranium(IV), i.e. to $Ca_9Nd_{0.5}U_{0.5}(PO_4)_{4.5}(SiO_4)_{1.5}F_2$. This extrapolation leads to $a = 9.404$ Å and $c = 6.904$ Å ($V = 528.7$ Å^3) which appears in very good agreement with the results obtained for (Nd, U)-britholite pellets. In these conditions, the coupled substitution $(Nd^{3+}, PO_4^{3-}) \Longleftrightarrow (Th^{4+} + U^{4+}, SiO_4^{4-})$ appears as a good way to be considered in the aim of the quantitative incorporation of tetravalent uranium in the britholite structure.

4. Conclusion

Unlike thorium that is quantitatively and easily incorporated in the britholite structure, the incorporation of tetravalent uranium appears rather difficult even after heating at high temperature. Indeed, only about 3.5 wt% of uranium are incorporated in the

Table 6
Refined unit cell parameters and volume of $Ca_9Nd_{0.5}Th_{0.5-z}U_z(PO_4)_{4.5}(SiO_4)_{1.5}F_2$ britholites ($0 < z < 0.5$)

Expected z	$\bar{z}$ (EPMA)	SiO_4/PO_4 (EPMA)	a (Å)	c (Å)	V (Å^3)	F_{20}
0	0	0.34 ± 0.02	9.413 (2)	6.9116 (15)	530.3 (4)	159 (0.0038; 33)
0.055	0.05	0.31 ± 0.02	9.415 (2)	6.9150 (15)	530.8 (4)	159 (0.0038; 33)
0.125	0.11	0.31 ± 0.02	9.412 (2)	6. 9132 (15)	530.4 (4)	135 (0.0045; 33)
0.25	0.26	0.35 ± 0.01	9.410 (2)	6.9097 (15)	529.9 (4)	148 (0.0041; 33)
0.375	0.32	0.34 ± 0.01	9.408 (2)	6.9085 (15)	529.5 (4)	202 (0.0030; 33)
0.5*	0.42	0.36 ± 0.02	9.404 (2)	6.9051 (15)	528.8 (4)	202 (0.0038; 26)

* Sample obtained after compaction of the reagents, calcination at 1400 °C for 6 h, polishing and finally grinding.

britholite structure when using a manual grinding of the initial mixture instead of 10.3 wt% expected. This incorporation rate being significantly improved (up to 5.9 wt%) when using mechanical grinding steps, the optimal grinding conditions were fixed to 15 min and 30 Hz for the frequency of oscillations.

All the samples considered are found to be composed by (Nd, U)-britholite and the calcium uranate CaU_2O_{5+y}. The formation of this latter compound appears as a consequence of the redox properties of uranium during the heating treatment. Indeed, solid state reaction between UO_2 and CaO leads to the formation of the intermediate $CaUO_4$ above 800 °C (thus to the oxidation of uranium even under inert atmosphere). Above 1100 °C, $CaUO_4$ is transformed into CaU_2O_{5+y} (which reaction is associated to the partial reduction of uranium above this temperature). Simultaneously, the incorporation of uranium(IV) in the (Nd, U)-britholite remains partial whatever the temperature considered even though it is significantly increased at 1400 °C. It probably proceeds through diffusion mechanism as confirmed when extending the heating time at this temperature. On the basis of these results, it clearly appears that the problems occurring during the incorporation of tetravalent uranium mainly result from the redox properties of this element (contrarily to thorium which remains in its tetravalent oxidation state). On the contrary, steric considerations associated to the smaller ionic radius of tetravalent uranium ($^{VII}r^{3+}_{Nd} = 1.05$ Å, $^{VII}r^{4+}_{Th} = 1.00$ Å and $^{VII}r^{4+}_{U} = 0.95$ Å [52]) would not be considered as the limiting factor in the uranium incorporation.

Two main methods can be developed to increase the incorporation of uranium in (Nd, U)-britholites. The first one deals with the compaction of the powdered initial mixture prior to perform the heating treatment at 1400 °C. In such conditions, the experimental uranium weight loading is almost equal to that expected and the formation of CaU_2O_{5+y} is only located at the surface of the pellet or inside the open pores. The second way is based on the simultaneous incorporation of thorium and uranium(IV), leading to the formation of (Nd, Th, U)-britholites $Ca_9Nd_{0.5}Th_{0.5-z}U_z(PO_4)_{4.5}(SiO_4)_{1.5}F_2$. It allows to prepare samples free of CaU_2O_{5+y} for low uranium weight loadings (typically for $z \leqslant 0.125$) while the formation of this secondary phase is significantly reduced for $z \geqslant 0.25$.

Rather similar redox considerations should be also carefully considered in the field of the incorporation of the two other actinides stabilized in the tetravalent oxidation state: i.e. neptunium and plutonium. Indeed, neptunium could be submitted to redox reactions rather similar to that observed for tetravalent uranium while plutonium could be reduced in its trivalent oxidation state when synthesizing (Nd, Pu)-britholites as already described in other phosphate-based ceramics [53–55] For this reason, the two methods developed in this work (initial compaction of the powder or simultaneous incorporation of thorium) could become of strong interest in order to prevent such redox problems.

Acknowledgements

This work was financially and scientifically supported by the French Research Group NOMADE (GdR 2023, CNRS/CEA/COGEMA). The authors are grateful to Johan Ravaux and Alain Kolher from LCSM (Université Henri Poincaré Nancy-I, France) for performing EPMA and SEM observations, and to Thérèse Lhomme from CREGU (Université Henri Poincaré Nancy-I, France) for her extensive help during the characterization of the samples by the μ-Raman technique.

References

[1] X. Deschanels, Evaluation de la faisabilité technique des nouvelles matrices de conditionnement des radionucléides à vie longue, Technical report, CEA/DTCD/2004/5, 2004.
[2] C. Guy, F. Audubert, J.E. Lartigue, C. Latrille, T. Advocat, C. Fillet, C. R. Phys. 3 (2002) 827.
[3] N. Dacheux, N. Clavier, A.C. Robisson, O. Terra, F. Audubert, J.E. Lartigue, C. Guy, C. R. Chim. 7 (2004) 1141.
[4] J.M. Montel, J.L. Devidal, D. Avignant, Chem. Geol. 191 (2002) 89.
[5] O. Terra, N. Clavier, N. Dacheux, R. Podor, New J. Chem. 27 (2003) 957.
[6] R. Podor, M. Cuney, C. Nguyen Trung, Am. Miner. 80 (1995) 1261.
[7] N. Dacheux, B. Chassigneux, V. Brandel, P. Le Coustumer, M. Genet, G. Cizeron, Chem. Mater. 14 (2002) 2953.
[8] P. Benard, V. Brandel, N. Dacheux, S. Jaulmes, S. Launay, C. Lindecker, M. Genet, D. Louër, M. Quarton, Chem. Mater. 8 (1996) 181.
[9] N. Clavier, N. Dacheux, G. Wallez, M. Quarton, J. Nucl. Mater. 352 (2006) 209.
[10] N. Dacheux, R. Podor, B. Chassigneux, V. Brandel, M. Genet, J. Alloy. Comp. 271 (1998) 236.
[11] N. Dacheux, A.C. Thomas, V. Brandel, M. Genet, J. Nucl. Mater. 257 (1998) 108.
[12] N. Dacheux, N. Clavier, J. Ritt, J. Nucl. Mater. 349 (2006) 291.
[13] N. Clavier, E. Du Fou de Kerdaniel, N. Dacheux, P. Le Coustumer, R. Drot, J. Ravaux, E. Simoni, J. Nucl. Mater. 349 (2006) 304.

[14] N. Clavier, N. Dacheux, P. Martinez, E. Du Fou de Kerdaniel, L. Aranda, R. Podor, Chem. Mater. 16 (2004) 3357.
[15] N. Clavier, N. Dacheux, R. Podor, Inorg. Chem. 45 (2006) 220.
[16] O. Terra, N. Dacheux, F. Audubert, R. Podor, J. Nucl. Mater. 352 (2006) 224.
[17] O. Terra, F. Audubert, N. Dacheux, C. Guy, R. Podor, J. Nucl. Mater. 354 (2006) 49.
[18] J. Carpéna, F. Audubert, D. Bernache-Assollant, L. Boyer, B. Donazzon, J.L. Lacout, N. Senamaud, Mat. Res. Soc. Symp. Proc. 506 (1998) 543.
[19] V. Sère, Géochimie des minéraux néoformés à Oklo (Gabon), histoire géologique du bassin d'Oklo: une contribution pour les études de stockages géologiques de déchets radioactifs, PhD thesis, University of Paris VII, 1996.
[20] R. Bros, J. Carpéna, V. Sère, A. Beltritti, Radiochim. Acta 74 (1996) 277.
[21] J. Carpéna, J.R. Kienast, K. Ouzegane, C. Jehanno, Geol. Soc. Amer. Bull. 100 (1988) 1237.
[22] J. Carpéna, in: P. Van den Haute, F. de Corte (Eds.), Advances in Fission Track Geochronology, Kluwer Academic, 1998, p. 81.
[23] S. Soulet, J. Carpéna, J. Chaumont, J.C. Krupa, M.O. Ruault, J. Nucl. Mater. 299 (2001) 227.
[24] L. Boyer, Synthèses et caractérisations d'apatites phosphosilicatées aux terres rares: application au nucléaire, PhD thesis, INP Toulouse, 1998.
[25] L. Boyer, J.-M. Savariault, J. Carpéna, J.-L. Lacout, Acta Crystallogr. C 54 (1998) 1057.
[26] F. Audubert, D. Bernache-Assolant, in: P. Vincenzini (Ed.), Advances in Science and Technology – Proceedings of the 10th International Ceramics Congress-CIMTEC 2002, Part B, Faenza, Italy, 31 (2002) 61.
[27] O. Fujino, S. Umetani, E. Ueno, K. Shigeta, T. Matsuda, Anal. Chim. Acta 420 (2000) 65.
[28] P.W. Reiners, K.A. Farley, Earth Planet. Sci. Lett. 188 (2001) 413.
[29] M. Jolivet, T. Dempser, R. Cox, C. R. Geosci. 335 (2003) 899.
[30] G. Engel, Mat. Res. Bull. 13 (1978) 43.
[31] J. Rakovan, R.J. Reeder, E.J. Elzinga, D.J. Cherniak, C.D. Tait, D.E. Morris, Environ. Sci. Technol. 36 (2002) 3114.
[32] E.R. Vance, M.L. Carter, B.D. Begg, R.A. Day, S.H.F. Leung, Mat. Res. Soc. Symp. Proc. 608 (2000) 431.
[33] E.R. Vance, C.J. Ball, B.D. Begg, M.L. Carter, R.A. Day, G.J. Thorogood, J. Am. Ceram. Soc. 86 (2003) 1223.
[34] R. El Ouenzerfi, M.T. Cohen-Adad, C. Goutardier, G. Panczer, Solid State Ionics 176 (2004) 225.
[35] F. Audubert, Private communication.
[36] O. Terra, Immobilisation d'actinides tétravalents dans trois matrices phosphatées : britholite, monazite et β-PDT, PhD thesis, IPNO T-05-03, University of Paris-Sud-11, 2005.
[37] A. Pialoux, B. Touzelin, J. Nucl. Mater. 255 (1998) 14.
[38] N. Dacheux, V. Brandel, M. Genet, New J. Chem. 19 (1995) 15.
[39] N. Dacheux, V. Brandel, M. Genet, New J. Chem. 19 (1995) 1029.
[40] N Dacheux, Matrices à base de phosphate d'uranium et de thorium: synthèses, caractérisations et lixiviation, PhD thesis, IPNO T-95-04, University of Paris-Sud-11, 1995.
[41] C. Keller, K.H. Walter, J. Inorg. Nucl. Chem. 25 (1965) 1253.
[42] N. Dacheux, R. Podor, V. Brandel, M. Genet, J. Nucl. Mater. 252 (1998) 179.
[43] R. Podor, Eur. J. Mineral. 7 (1995) 1353.
[44] N. Clavier, Elaboration de Phosphate–Diphosphate de Thorium et d'Uranium (β-PDTU) et de matériaux composites β-PDTU/monazite à partir de précurseurs cristallisés. Etudes du frittage et de la durabilité chimique, PhD thesis, IPNO T-04-15, University of Paris-Sud-11, 2004.
[45] R. El Ouenzerfi, C. Goutardier, G. Panczer, B. Moine, M.T. Cohen-Adad, M. Trabelsi-Ayedi, N. Kbir-Ariguib, Solid State Ionics 156 (2003) 209.
[46] R.W.G. Syme, D.J. Lockwood, H.J. Ken, Solid State Phys. 10 (1977) 1335.
[47] T. Hirata, E. Asari, M. Kitajima, J. Solid State Chem. 110 (1994) 201.
[48] V. Brandel, N. Dacheux, M. Genet, R. Podor, J. Solid State Chem. 159 (2001) 139.
[49] R.L. Frost, M.L. Weier, W. Martens, J. Cejka, Vib. Spectrosc. 41 (2006) 205.
[50] R.L. Frost, M.L. Weier, Spectrochim. Acta A 60 (2004) 2399.
[51] A.C. Thomas, N. Dacheux, P. Le Coustumer, V. Brandel, M. Genet, J. Nucl. Mater. 295 (2001) 249.
[52] R.D. Shannon, Acta Crystallogr. A 32 (1976) 751.
[53] D. Bregiroux, R. Belin, P. Valenza, F. Audubert, D. Bernache-Assolant, J. Nucl. Mater., in press, doi:10.1016/j.jnucmat.2006.12.042.
[54] D. Bregiroux, R. Belin, F. Audubert, D. Bernache-Assolant, in: R. Alvarez, N.D. Bryan, I. May (Eds.), Recent Advances in Actinides Science, RSC Publishing, 2006, p. 749.
[55] D. Bregiroux, Synthèse par voie solide et frittage de céramiques à structure monazite. Application au conditionnement des actinides mineurs, PhD thesis no. 59-2005, University of Limoges, 2005.